

Supporting Information

Proton Transfers to DNA in Native Electrospray Ionization Mass Spectrometry: A Quantum Mechanics/Molecular Mechanics Study

Mirko Paulikat^a, Juan Aranda^b, Emiliano Ippoliti^a, Modesto Orozco^{b,c,}, Paolo Carloni^{a,d,*}*

^aComputational Biomedicine (IAS-5/INM-9), Forschungszentrum Jülich GmbH, Wilhelm-Johnen-Straße, 52428 Jülich, Germany

^bInstitute for Research in Biomedicine (IRB) Barcelona, The Barcelona Institute of Science and Technology, Baldori Reixac 10, 08028 Barcelona, Spain

^cDepartment of Biochemistry and Biomedicine, University of Barcelona, Avinguda Diagonal 645, 08028, Spain

^dDepartment of Physics, RWTH Aachen University, Otto-Blumenthal-Straße, 52062 Aachen, Germany

* Email: modesto.orozco@irbbarcelona.org, p.carloni@fz-juelich.de

1. Calculated Properties and Definitions

Let us consider an atom i , either the NH_4^+ -nitrogen atom (N_{Amm}) or the DMP/ heptanucleotide phosphorus atom ($\text{P}_{\text{DMP}}/\text{P}_{\text{DNA}}$) coordinated by a group of atoms j (water oxygens (O_{Wat})). Then, the hydration number for atom (i) reads:

$$HN(i) = \sum_j \frac{1 - \left(\frac{r_{ij} - d_0}{r_0}\right)^6}{1 - \left(\frac{r_{ij} - d_0}{r_0}\right)^{12}} \quad (1)$$

where r_{ij} corresponds to the distance between atoms i and j . The parameters d_0 and r_0 are chosen in the way that only the first peak of the $\text{N}_{\text{Amm}}-\text{O}_{\text{Wat}}$ or the $\text{P}_{\text{DMP/DNA}}-\text{O}_{\text{Wat}}$ radial distribution functions is fully included. If $i = \text{N}_{\text{Amm}}$, $d_0 = 3.0 \text{ \AA}$ and $r_0 = 1.0 \text{ \AA}$ (Fig. S1a), if $i = \text{P}_{\text{DMP}}$, $d_0 = 3.7 \text{ \AA}$ and $r_0 = 1.0 \text{ \AA}$ (Fig. S1b). If $i = \text{P}_{\text{DNA}}$, d_0 and r_0 have identical values (see Fig. S1c).

We employed the GROMACS `hbond` module to determine the number of internal hydrogen bonds of the heptanucleotide.^{1,2} Cutoffs of 3 \AA and 150° was used for the hydrogen-acceptor distance and the donor-hydrogen-acceptor angle.

We defined the ammonium and the anions if the distance between N_{Amm} and P_{DMP} is 4 \AA or lower (in the case of DMP) or the distance between N_{Amm} and any P_{DNA} is 4 \AA or lower (in the case of the heptamer).

The definition of the collective variable (CV) for all umbrella sampling (US) performed here is shown in Chart S1.

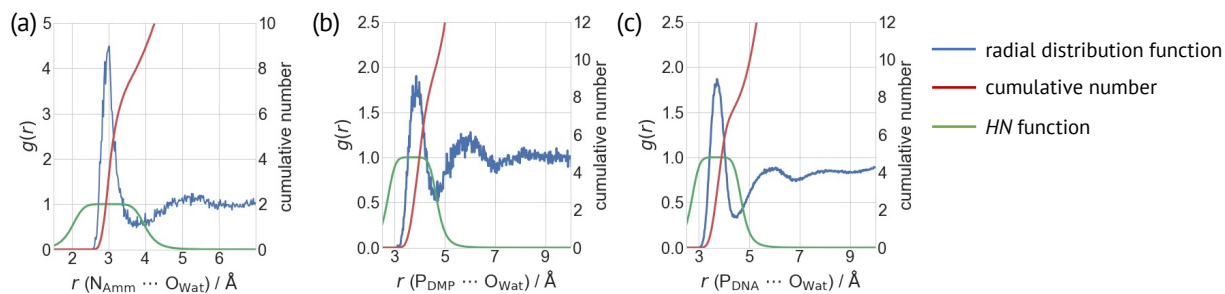


Figure S1: Radial distribution functions $g(r)$, cumulative number and summand of equation (1).

(a) $N_{\text{Amm}}\text{-}O_{\text{Wat}}$ $g(r)$. (b) $P_{\text{DMP}}\text{-}O_{\text{Wat}}$ $g(r)$. (c) $P_{\text{DMP}}\text{-}O_{\text{Wat}}$ $g(r)$.

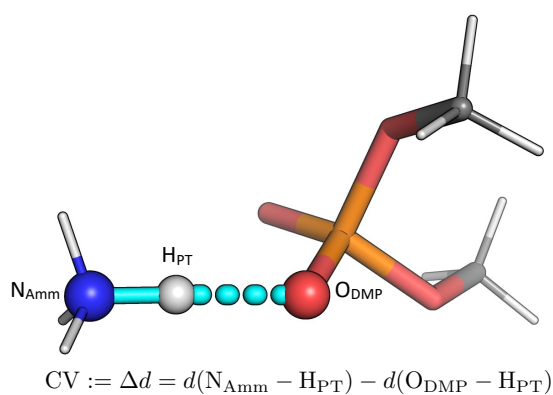


Chart S1.

2. Results: Additional Details

2.1 MD of I in aqueous solution

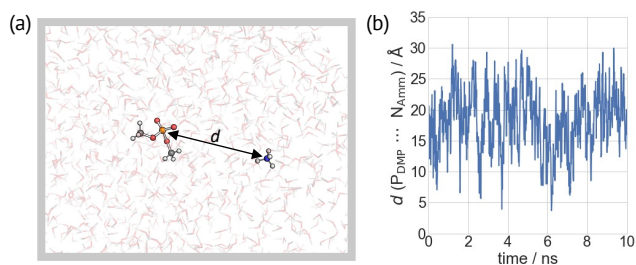


Figure S2: (a) Snapshot of **I** in solution, highlighting the $P_{\text{DMP}} - N_{\text{Amm}}$ distance d . (b) d plotted as a function of simulated time.

2.2 MD of I in aqueous droplets

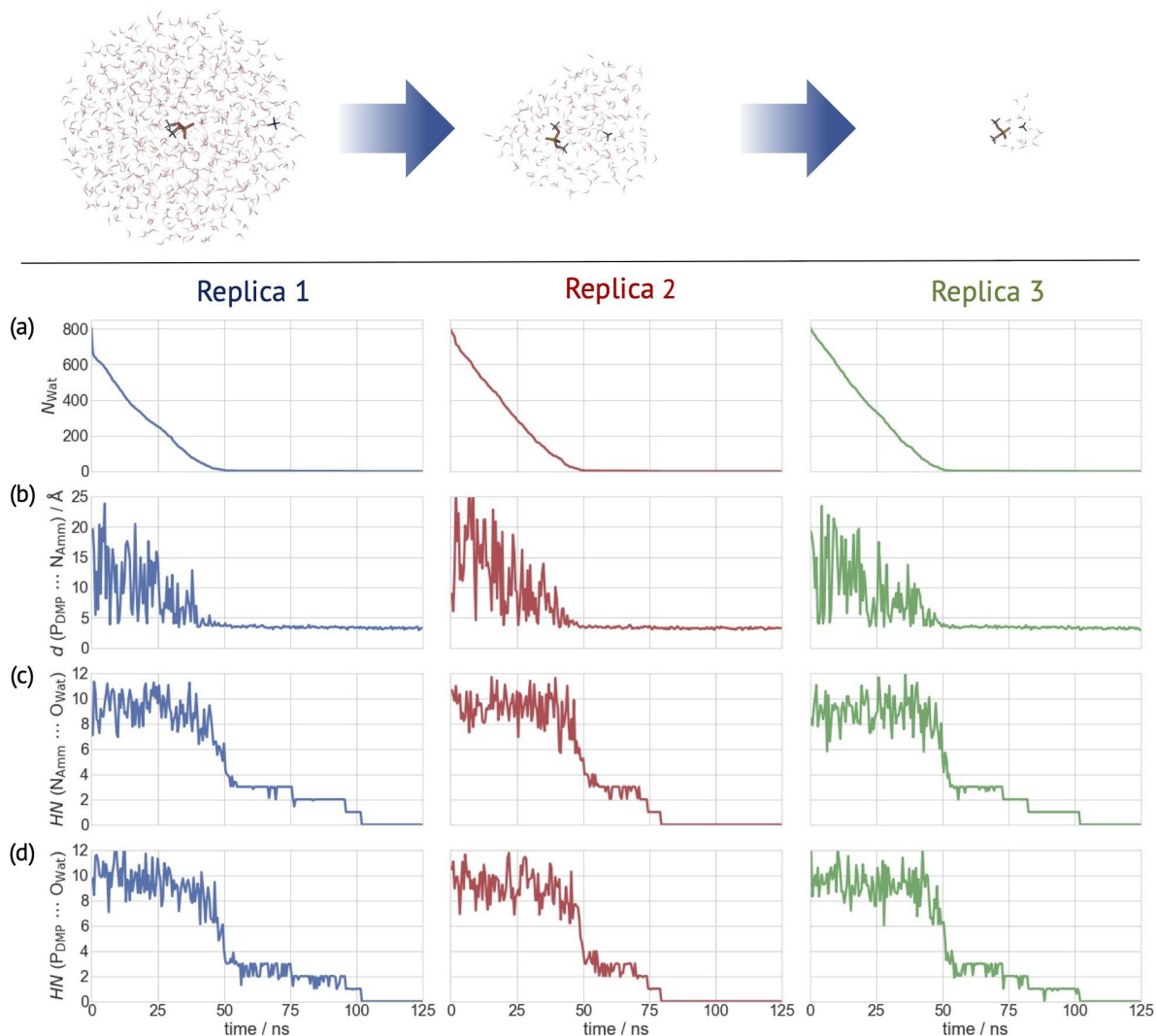


Figure S3: Top: Evaporation process of the dimethyl phosphate ion and an ammonium ion in a water droplet as observed during one of our three replicas of the simulation. **Bottom:** Selected properties of the three replicas of gas phase MD simulations plotted as a function of time: **(a)** Number of water molecules in the system (N_{Wat}). **(b)** $\text{P}_{\text{DMP}} - \text{N}_{\text{Amm}}$ distance; **(c)–(d)** $HN(i)$ ($i = \text{N}_{\text{Amm}}$ **(c)** and P_{DMP} **(d)**).

2.3 QM/MM of I in the Gas Phase

We report here the results from 2.42 ps QM/MM MD simulations of **Ia-c**.

The simulation of **Ia** leads readily to proton transfer. The resulting neutral state is stable with $HN \sim 2-3$ for the rest of the dynamics ($d(N_{\text{Amm}}-\text{H}_{\text{PT}}) = 1.4 \pm 0.2 \text{ \AA}$, $d(\text{O}_{\text{DMP}}-\text{H}_{\text{PT}}) = 1.2 \pm 0.1 \text{ \AA}$).

In the QM/MM MD of the other two complexes, the ammonium ion is more hydrated ($HNs \sim 3-4$ and $4-6$). No proton transfer is observed. The N-H bond forming an H-bond with DMP ion increases by $\sim 0.1 \text{ \AA}$ relative to the others (see Fig. S4).

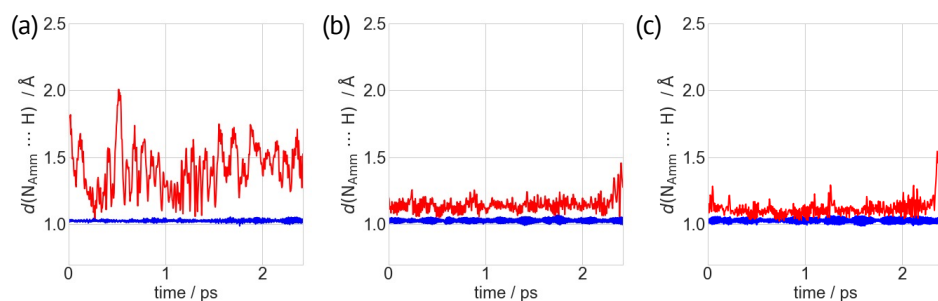


Figure S4: $N_{\text{Amm}}-\text{H}$ bond distances of gas phase QM/MM-MD simulations plotted as a function of time for systems (a) **Ia**, (b) **Ib** and (c) **Ic**. The N-H bond involved in the proton transfer is shown in red, while the other N-H bonds are shown in blue.

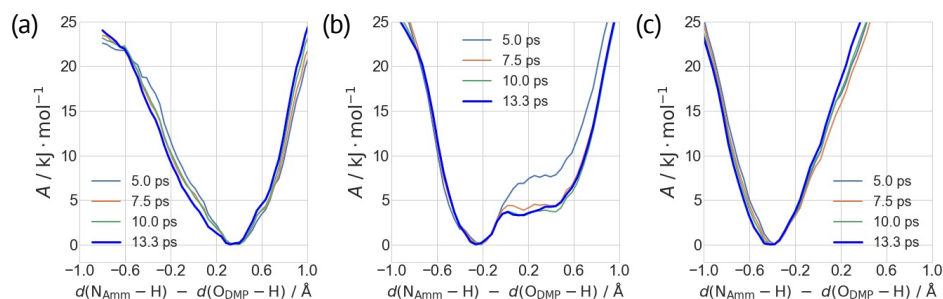


Figure S5: Time evolution of the free energy profiles as a function of the difference of the breaking/forming $N_{\text{Amm}}-\text{H}$ and $\text{H}-\text{O}_{\text{DMP}}$ bond distances for systems (a) **Ia**, (b) **Ib** and (c) **Ic**.

2.4 MD of II in water solution

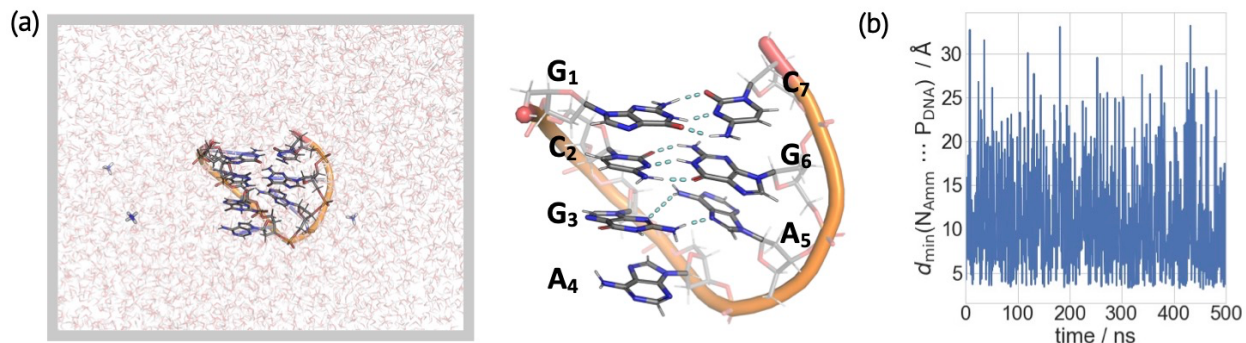


Figure S6 (a) MD snapshot of complex II in aqueous solution, showing the hairpin structure of the heptanucleotide and 6 NH₄⁺ ions. Inset: zoom on the structure of the heptanucleotide. The H-bonds between base pairs are shown as cyan, dashed lines. (b) $P_{\text{DNA}}-N_{\text{Amm}}$ distance d plotted as a function of time.

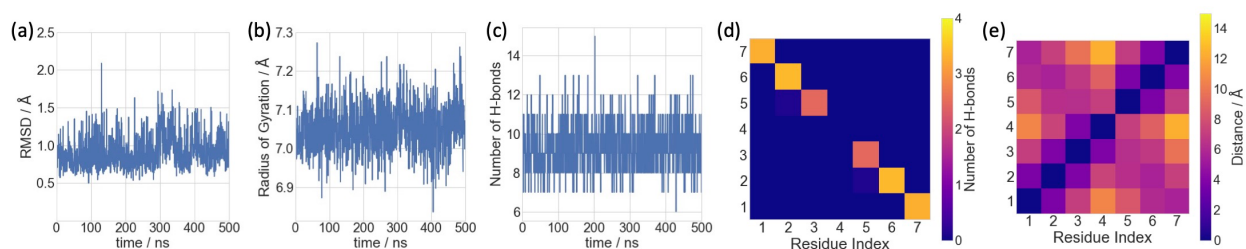


Figure S7: (a)–(c) Selected structural descriptors of the heptanucleotide plotted as a function of simulated time. (a) Root-mean-square-deviation (RMSD) of all atoms relative to the initial structure. (b) Radius of gyration. (c) Total number of internal H-bonds. (d) Heatmap of the average number of observed hydrogen bonds between the base pairs, reflecting the formation of two canonical base pairs (G₁-C₇ and C₂-G₆ with ~3 H-bonds) and one non-canonical base pair (G₃-A₅ with ~2 H-bonds). (e) Contact map of the nucleobases, showing the characteristic X-shape of an antiparallel duplex.³

2.5 MD of II in the water droplets

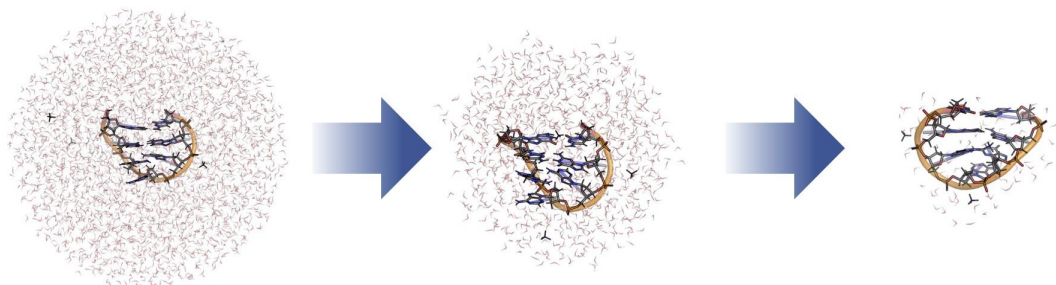


Figure S8: Evaporation process of the heptanucleotide and ammonium ions in a water droplet as observed in one of the 225 ns MD simulations performed here.

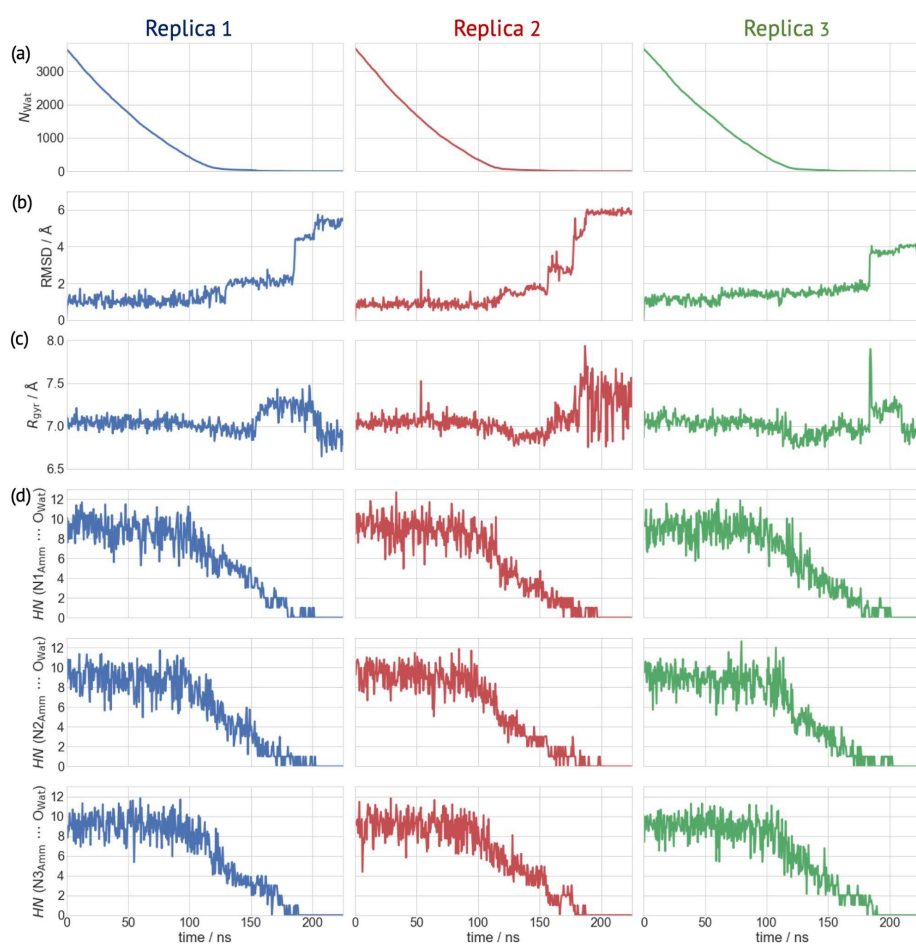


Figure S9: Selected properties plotted as a function of simulated time in the three replicas of gas phase MD simulations. (a) Number of water molecules (N_{Wat}). (b) RMSD of heptanucleotide's all atoms relative to the initial structure. (c) R_{gyr} . (d) HN of the three ammonium ions.

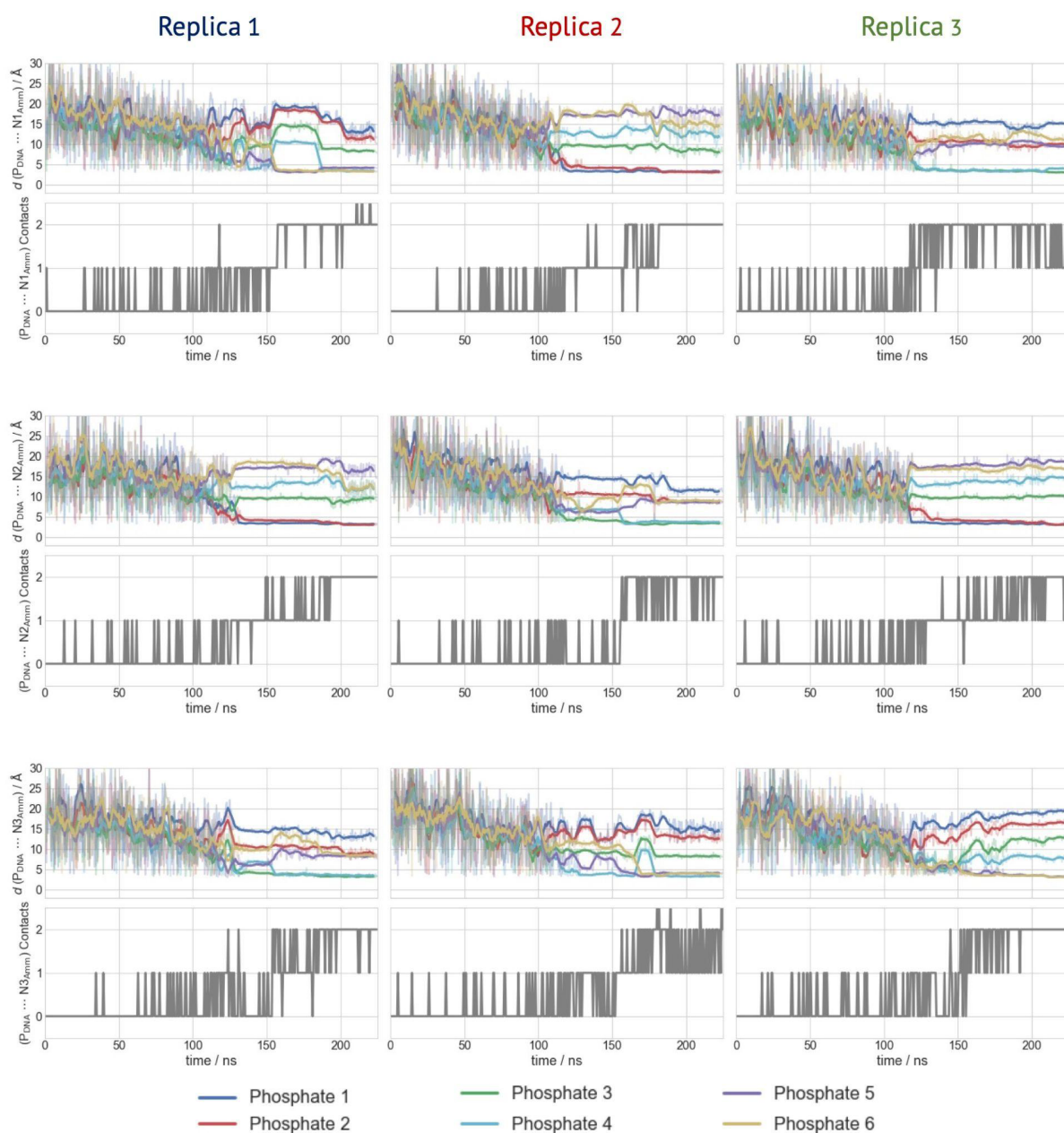


Figure S10: Distances d between P_{DNA} and the three N_{Amm} -atoms from the three MD replicas. Data at the end of each 500 ps batch of MD simulations are shown as transparent lines, while their moving averages (window size of 10) are represented as bold lines. The corresponding number of contacts are shown below each distance plot.

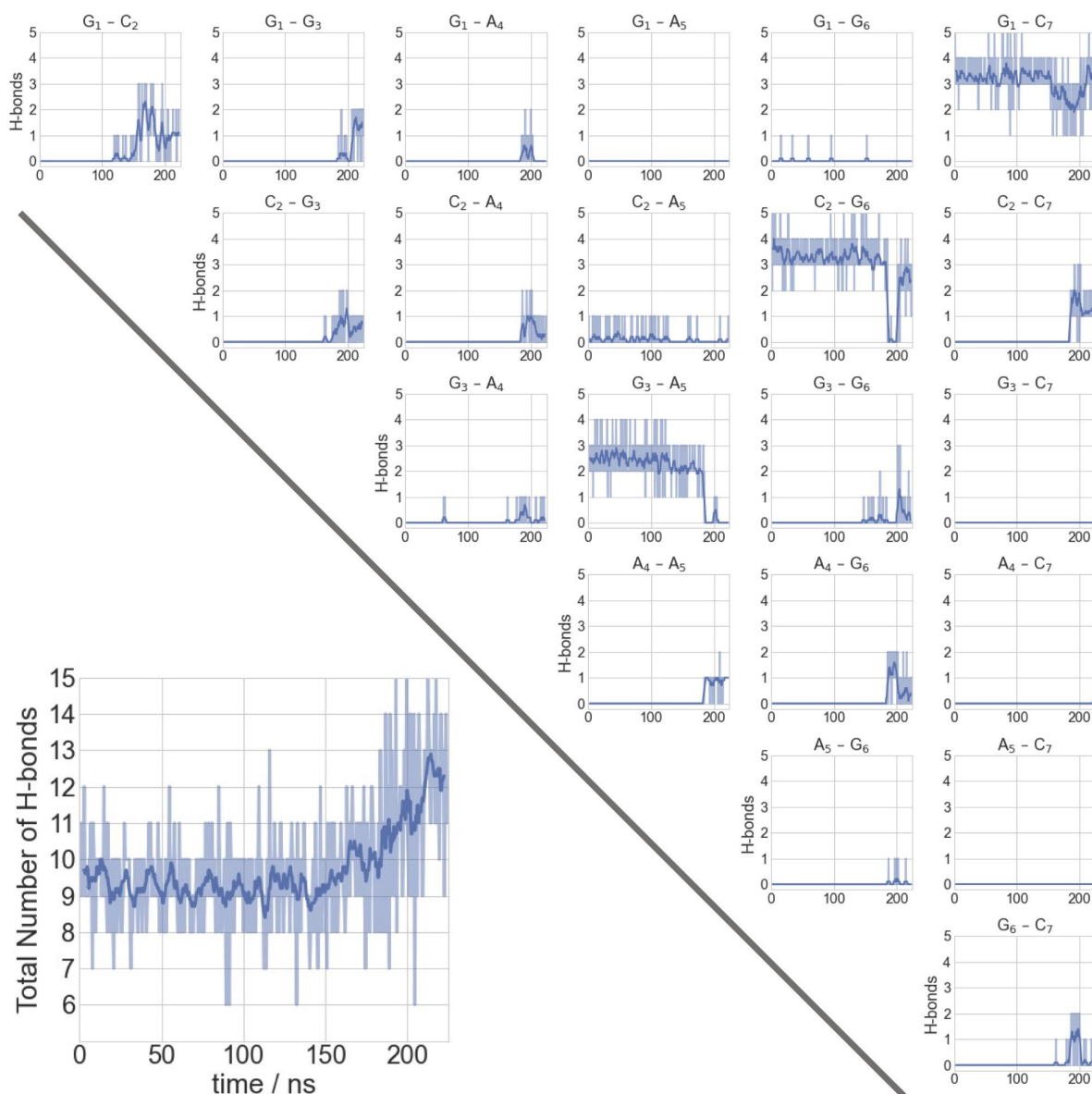


Figure S11: Nucleobase H-bond interactions plotted as a function of time (replica 1). Data at the end of each 500 ps batch of MD simulations are shown as transparent lines, while their moving averages (window size of 10) are represented as bold lines. Upper right: Base pair specific number of H-bonds. Lower left: Total number of H-bonds of the heptanucleotide.

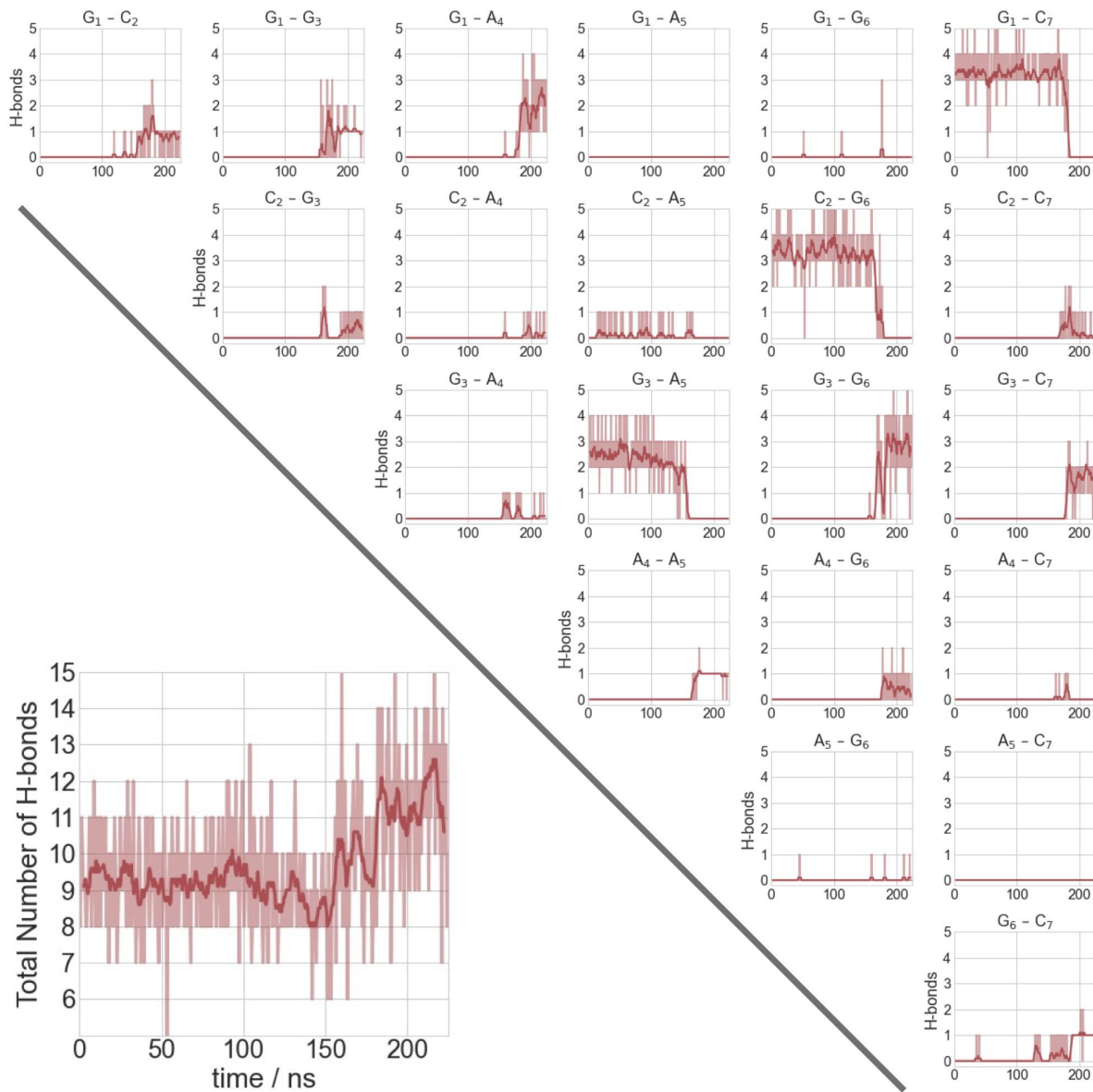


Figure S12: Same as Fig. S11 for the second replica of the MD.

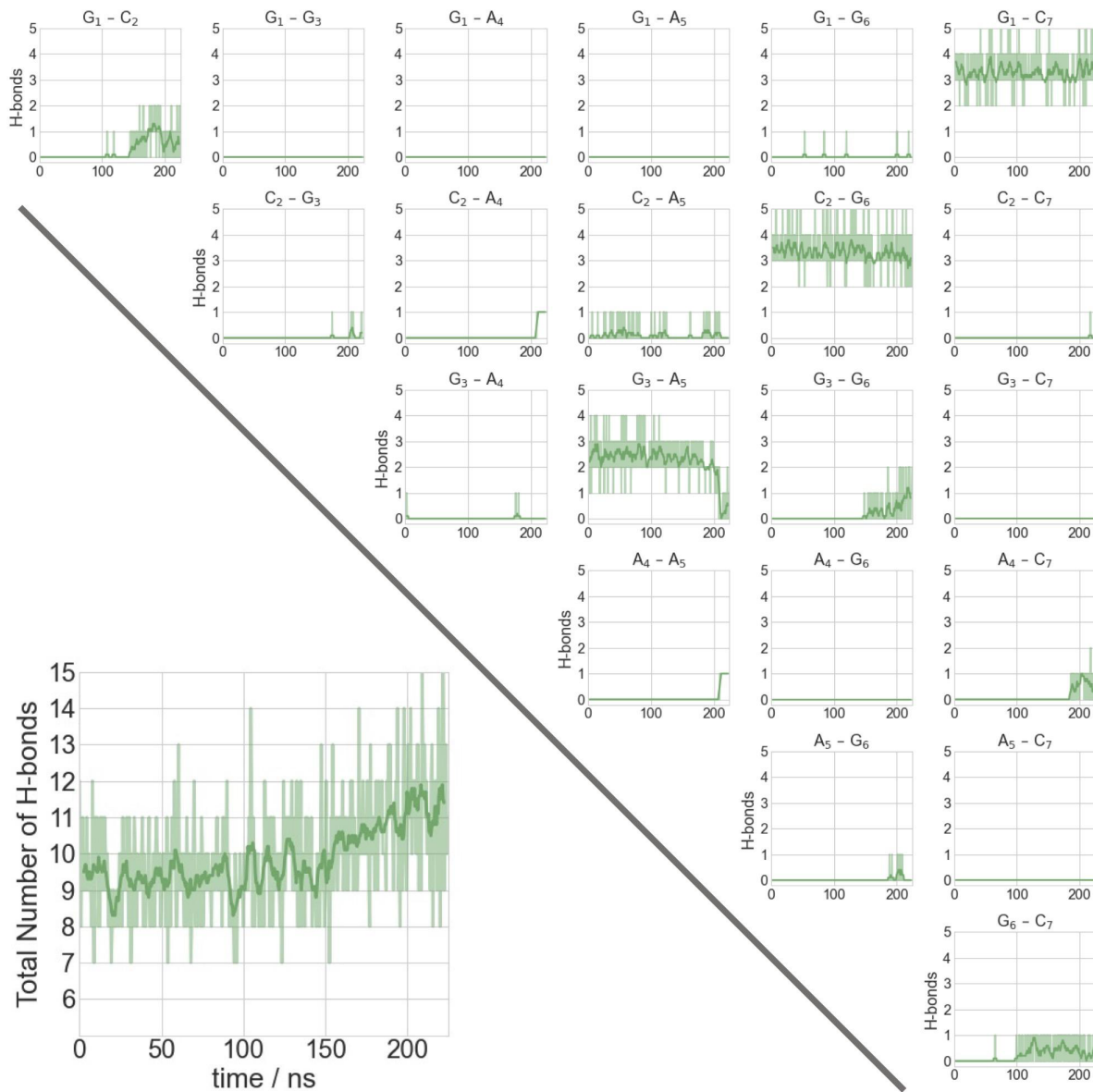


Figure S13: Same as Fig. S11 for the third replica of the MD.

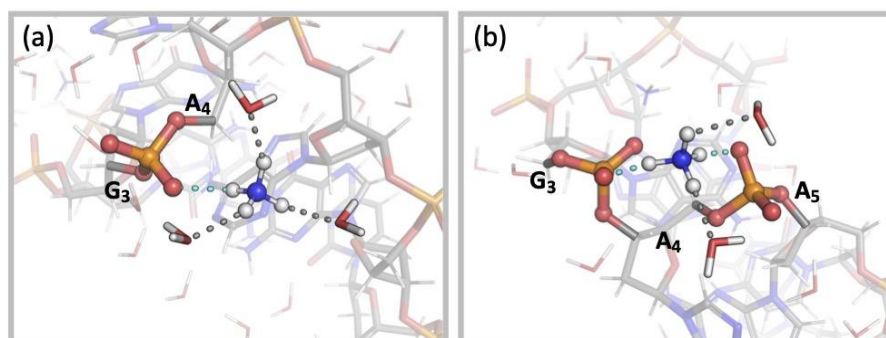


Figure S14: Salt bridges between a NH_4^+ ion with (a) one phosphate or (b) two phosphate groups as observed in our MD simulations.

2.6 QM/MM of II in the Dehydrated Water Droplet

2.6.1 Partitioning of the QM Region for the QM/MM Calculations.

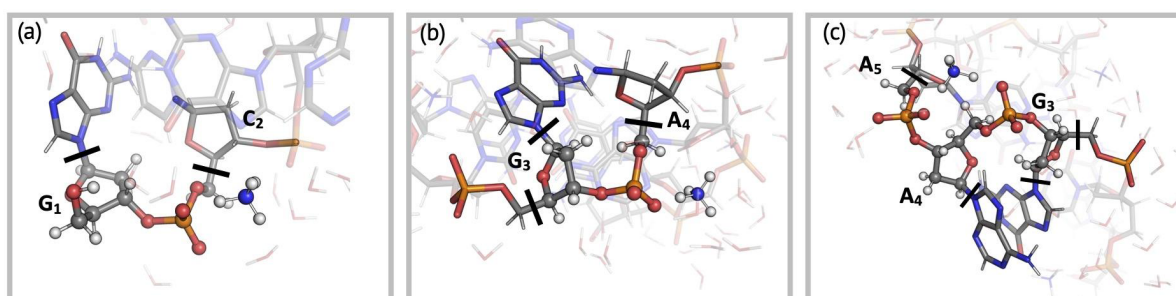


Figure S15: QM atoms (spheres) in the QM/MM calculations. Cut covalent bonds indicated as black lines.

2.6.2 QM/MM Simulations of Complexes IIa-j.

We performed 2.5 ps QM/MM MD and 25.0 ps QM/MM US calculations for each complex.

In the 2.5ps-long QM/MM MD of **IIa**, **IIb** and **IIc**, the ammonium ion forms a H-bond to the phosphodiester group between G₃ and A₄ (Fig. 4a), with different initial conditions (see Table 1). The NH_4^+ ion forms H-bonds to the O4'-deoxyribose and N3- adenine atoms of the A₅ residue of the heptanucleotide (Fig. 4a). In **IIa** and **IIb**, no proton transfer is observed. The N–H bond involved in the proton transfer is elongated to $1.2 \pm 0.1 \text{ \AA}$ (**IIa**) and $1.12 \pm 0.04 \text{ \AA}$ (**IIb**) relative to

the other bonds of the NH_4^+ ion ($\sim 1.05 \text{ \AA}$), while the O–H distance is $1.4 \pm 0.1 \text{ \AA}$ (**IIa**) and $1.5 \pm 0.1 \text{ \AA}$ (**IIb**). The ammonium HN fluctuates around $\sim 2\text{--}3$ (**IIa**) and $\sim 2\text{--}4$ (**IIb**). In **IIc**, the proton is almost shared between the two moieties. The N–H and O–H distances are observed to strongly fluctuate with $1.3 \pm 0.2 \text{ \AA}$ and $1.4 \pm 0.2 \text{ \AA}$. The NH_4^+ HN fluctuates around ~ 2 .

In **IIId** and **IIe**, the ammonium ion forms a H-bond to the phosphodiester group between G_1 and C_2 , with different initial conditions (Fig. 4b). No proton transfer is observed. The N–H bond is $1.12 \pm 0.05 \text{ \AA}$ (**IIId**) and $1.2 \pm 0.2 \text{ \AA}$ (**IIe**), while the O–H distance is $1.5 \pm 0.1 \text{ \AA}$ (**IIId**) and $1.2 \pm 0.1 \text{ \AA}$ (**IIe**). The NH_4^+ HN strongly fluctuates from $\sim 3\text{--}6$ (**IIId**) and $\sim 2\text{--}5$ (**IIe**). The NH_4^+ ion also forms a H-bond with N7-guanine atoms of the G_3 residue of the heptanucleotide (Fig. 4b).

In **IIIf**, the ammonium ion forms H-bonds to two phosphodiester groups of the moiety $G_3\text{--}p\text{--}A_4\text{--}p\text{--}A_5$ (Fig. 4c). No proton transfer is observed. The N–H bonds involved in H-bond interactions are just slightly elongated to about $1.09 \pm 0.04 \text{ \AA}$, while the O–H distances are $1.6 \pm 0.1 \text{ \AA}$. The NH_4^+ HN fluctuates around ~ 2 .

In **IIIg**, the same interaction mode as for **IIIf** is studied, but with different initial conditions (see Table 1). No proton transfer is observed. The ammonium interacts stronger with the $G_3\text{--}p\text{--}A_4$ group than with the $A_4\text{--}p\text{--}A_5$ group: The N–H bonds involved in H-bond with the phosphate groups are $1.2 \pm 0.1 \text{ \AA}$ and $1.1 \pm 0.1 \text{ \AA}$, respectively. The corresponding O–H distances are $1.5 \pm 0.2 \text{ \AA}$ and $1.7 \pm 0.3 \text{ \AA}$, respectively. The NH_4^+ HN fluctuates around $\sim 1\text{--}2$. The NH_4^+ ion features no other H-bond interactions with the heptanucleotide as in **IIIf**.

In **IIIf** exhibits the same interaction mode as for **IIIf** and **IIIg** but with different initial conditions (see Table 1). No proton transfer is observed. However, the ammonium interacts strongly with the $G_3\text{--}p\text{--}A_4$ group: The N–H and O–H bond lengths are very similar with $1.3 \pm 0.2 \text{ \AA}$ and $1.3 \pm 0.2 \text{ \AA}$, respectively. The interaction to the $A_4\text{--}p\text{--}A_5$ group leads to a slightly elongated N–H bond with

$1.07 \pm 0.04 \text{ \AA}$, while the O–H distance is $1.7 \pm 0.2 \text{ \AA}$. The NH_4^+ HN fluctuates around $\sim 0\text{--}2$. The NH_4^+ ion features no other H-bond interactions with the heptanucleotide.

III shows the same interaction of the NH_4^+ ion with the G1–p–C2 group as for **II d** and **II e**, but with different initial conditions (see Table 1). During the dynamics, the ammonium ion additionally forms a H-bond to the phosphodiester group between C₂ and G₃ (Fig. 4d). No proton transfer is observed. The N–H bond involved in proton transfer is $1.1 \pm 0.1 \text{ \AA}$, while the O–H distance is $1.5 \pm 0.1 \text{ \AA}$. The NH_4^+ HN varies from $\sim 2\text{--}5$.

In **II j**, the same interaction mode evolves as for **III** (Fig. 4d), but from different initial conditions (see Table 1). The N–H bond involved in proton transfer is elongated to $1.2 \pm 0.2 \text{ \AA}$ relative to the other bonds of the NH_4^+ ion ($\sim 1.05 \text{ \AA}$), while the O–H distance is $1.3 \pm 0.2 \text{ \AA}$. The NH_4^+ HN varies from $\sim 1\text{--}2$.

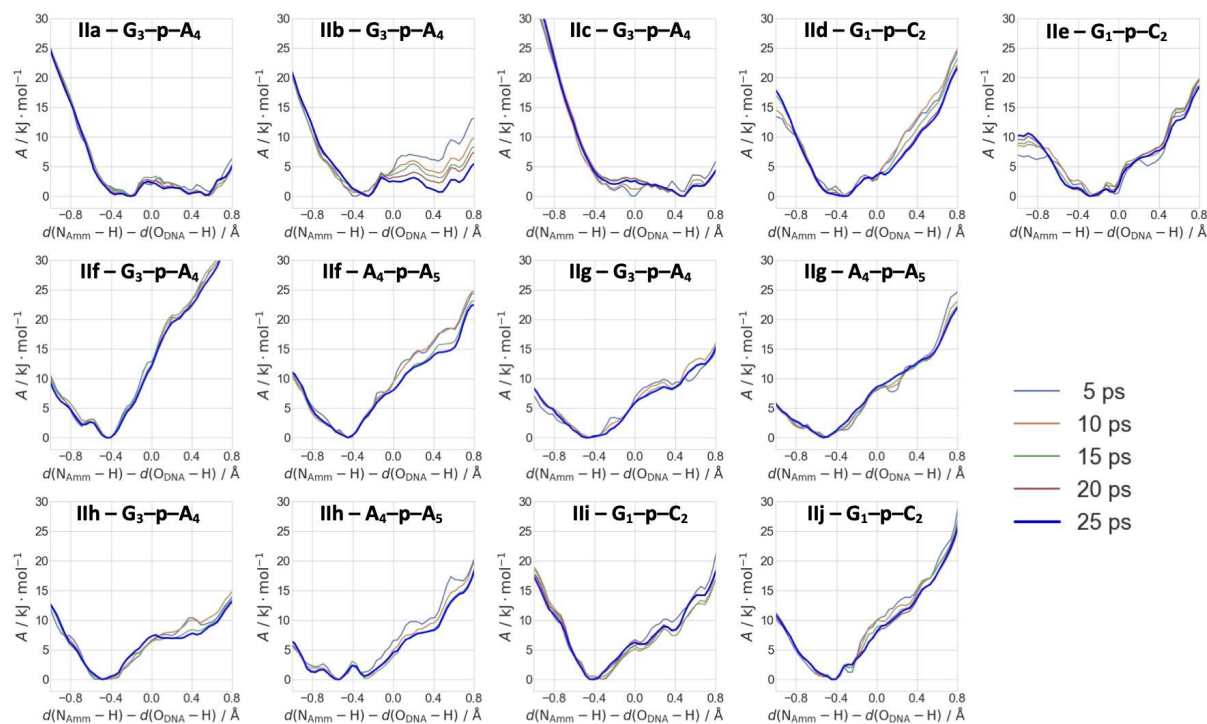


Figure S16: Time evolution of the free energy profiles as a function of the difference of the breaking/forming $N_{\text{Amm}}\text{-H}$ and H-O_{DNA} bond distances. Details on the systems and the interaction modes are described in the main text (see Fig. 4 and Table 1).

3. References

- (1) Abraham, M. J.; Murtola, T.; Schulz, R.; Páll, S.; Smith, J. C.; Hess, B.; Lindahl, E. GROMACS: High Performance Molecular Simulations through Multi-Level Parallelism from Laptops to Supercomputers. *SoftwareX* **2015**, *1*, 19–25.
- (2) van der Spoel, D.; Lindahl, E.; Hess, B.; Groenhof, G.; Mark, A. E.; Berendsen, H. J. C. GROMACS: Fast, Flexible, and Free. *J. Comput. Chem.* **2005**, *26*, 1701–1718.

(3) Arcella, A.; Dreyer, J.; Ippoliti, E.; Ivani, I.; Portella, G.; Gabelica, V.; Carloni, P.; Orozco, M. Structure and Dynamics of Oligonucleotides in the Gas Phase. *Angew. Chem. Int. Ed.* **2015**, *54*, 467–471.